CDK4/6 Inhibition Induces CD8⁺ T Cell Antitumor Immunity via MIF-Induced Functional Orchestration of Tumor-Associated Macrophages

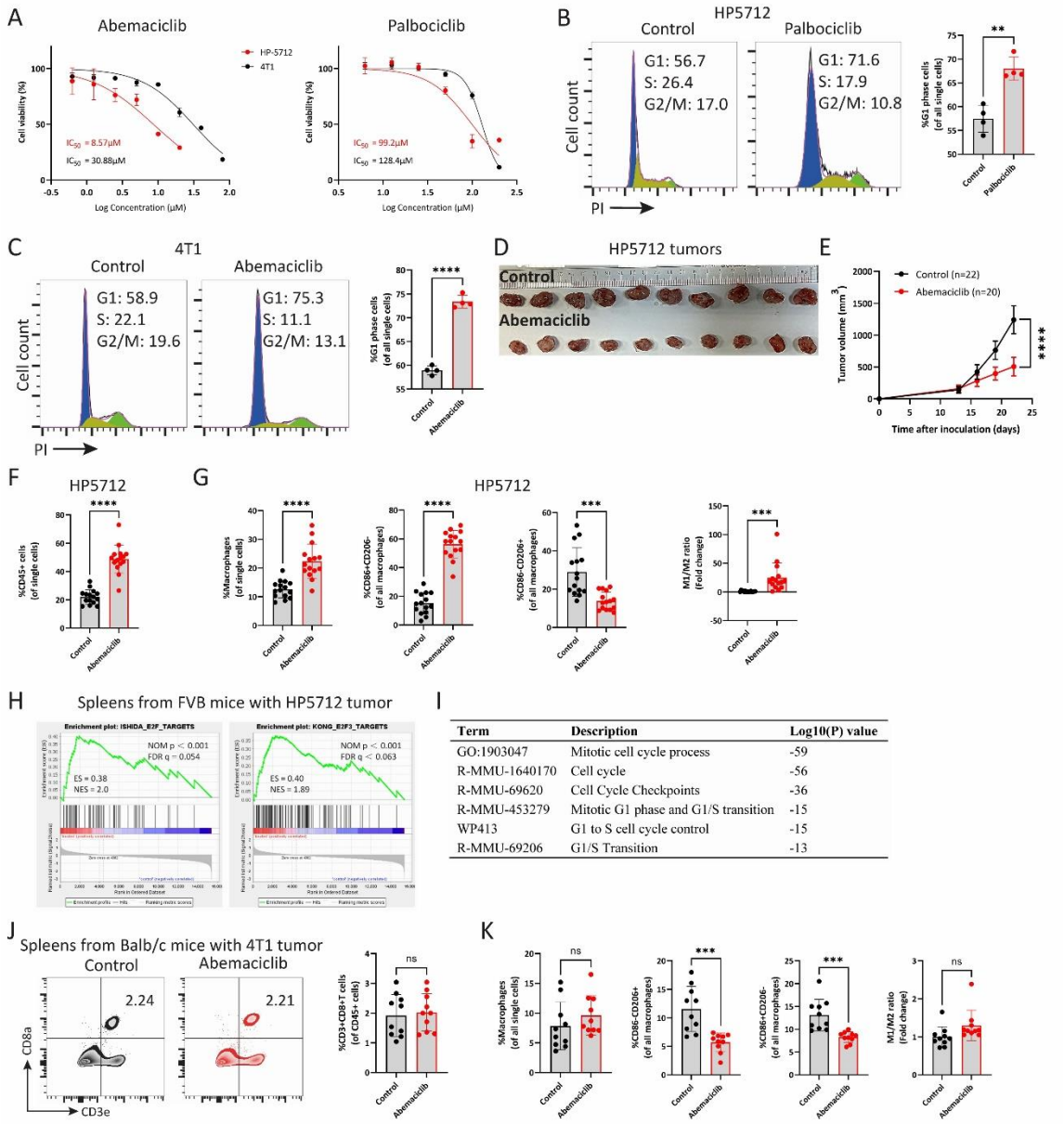

Term	Description	Log10(P) value
GO:1903047	Mitotic cell cycle process	-59
R-MMU-1640170	Cell cycle	-56
R-MMU-69620	Cell Cycle Checkpoints	-36
R-MMU-453279	Mitotic G1 phase and G1/S transition	-15
WP413	G1 to S cell cycle control	-15
R-MMU-69206	G1/S Transition	-13

Supplementary Figure 1. CDK4/6 inhibition creates an immunostimulatory status in the tumor microenvironment but not in the circulatory system.

A. IC50 of CDK4/6 inhibitors, Abemaciclib (left) and Palbociclib (right), in HP5712 and 4T1 cell lines.

B-C. Representative FACS cell cycle distribution and comparison of G1 phase cell populations of HP5712 (B) and 4T1 (C) cells after control or Abemaciclib treatment (n=4, respectively).

D. Representative tumor images of FVB mice orthotopically injected with HP5712 cells after 10 days of control or Abemaciclib treatment (n=10, respectively).

E. Tumor volume changes of FVB mice orthotopically injected with HP5712 cells after 10 days of control or Abemaciclib treatment (control, n=22; Abemaciclib, n=20).
F. Intratumoral lymphocytes from FVB mice orthotopically injected with HP5712 cells after 10 days of control or Abemaciclib treatment.
G. Intratumoral macrophages, M1 phenotypes, M2 phenotypes, and fold changes of M1/M2 ratio in FVB mice orthotopically injected with HP5712 cells after 10 days of control or Abemaciclib treatment (n=15, respectively).
H-I. GSEA terms (H) and GO terms (I) significantly upregulated by Abemaciclib compared to control in spleens from FVB mice orthotopically injected with HP5712 cells (n=3, respectively).
J. Representative FACS plot and quantifications of CD8+ T cells in spleens from Balb/c mice orthotopically injected with 4T1 cells after 10 days of control or Abemaciclib treatment (n=10, respectively).
K. Intratumoral macrophages, M1 phenotypes, M2 phenotypes, and fold changes of M1/M2 ratio in spleens from Balb/c mice orthotopically injected with 4T1 cells after 10 days of control or Abemaciclib treatment (n=10, respectively).
Unpaired two-tailed t-tests (B, C, E-G, J, K). Error bars represent SD. ns $p > 0.05$, **$p < 0.01$, ***$p < 0.001$, ****$p < 0.0001$.

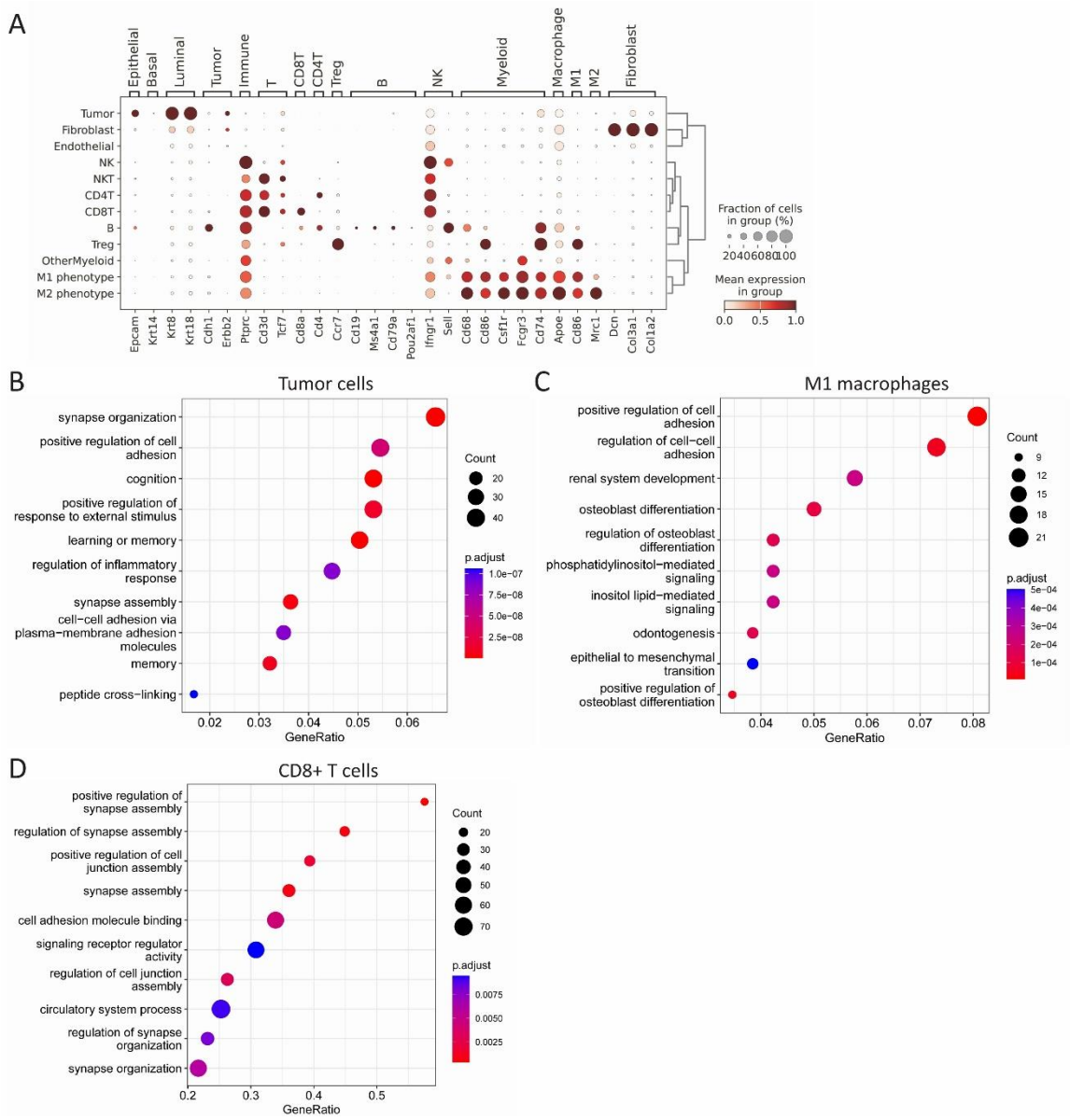

Supplementary Figure 2. Cell type annotation for scRNA-seq of Balb/c mice orthotopically implanted 4T1 tumors after control or Abemaciclib treatment.

A. Cell type annotation for scRNA-seq of tumors.

B-D. GO terms of Abemaciclib-upregulated genes in tumor cells (B), M1 macrophages (C), and CD8+ T cells (D) compared to control.

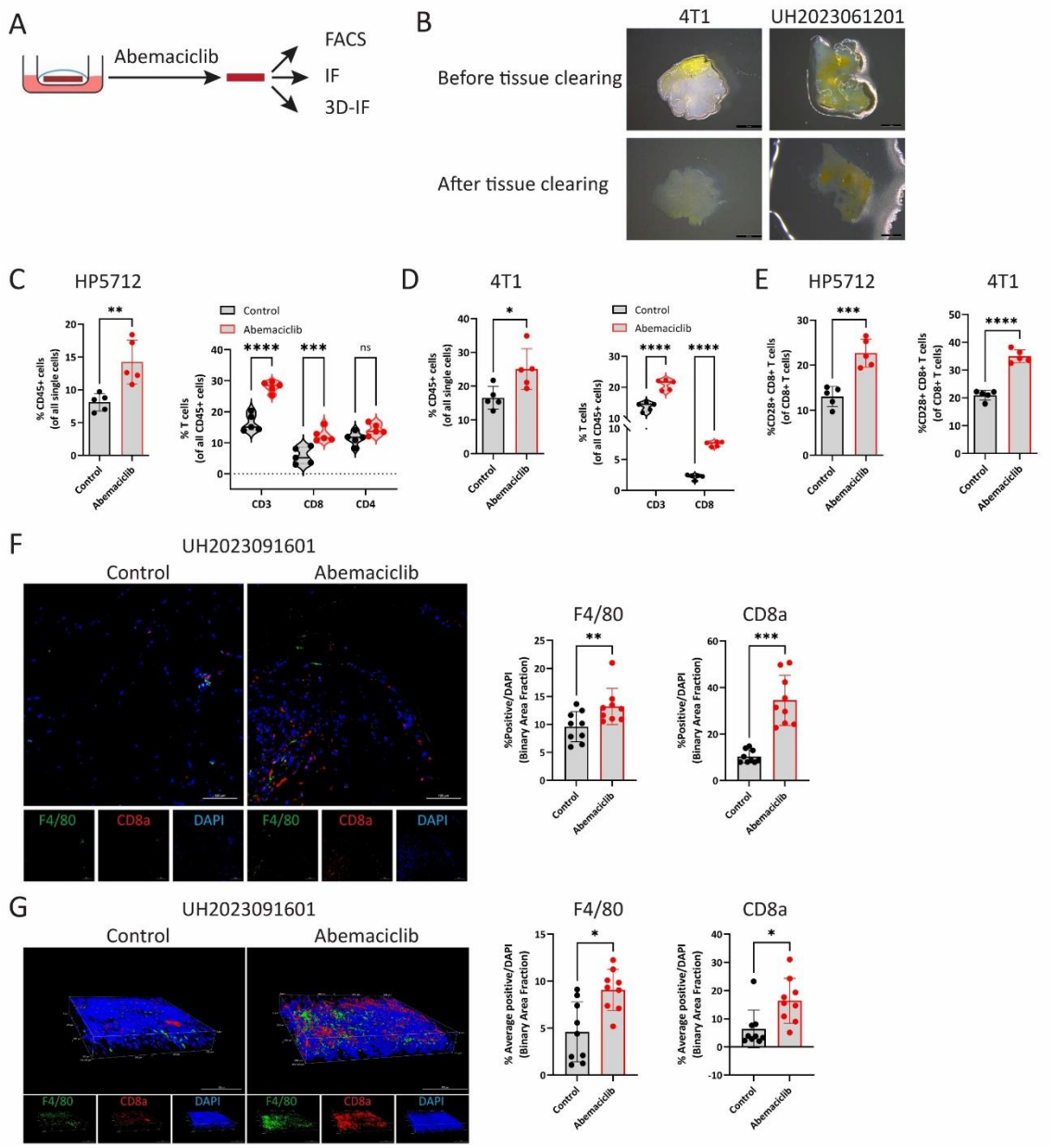

Supplementary Figure 3. CDK4/6 inhibition increases intratumoral CD8+ T cells and macrophages ex vivo.

A. Workflow of assessing the tumor immune cell changes of tumor slices after Abemaciclib treatment.

B. Representative images of murine and human tumor slices before and after tissue clearing; scale bar = 2 mm.

C-D. Intratumoral lymphocytes and T cell subpopulations in immunocompetent mice orthotopically injected with HP5712 tumor slices (C) or 4T1 tumor slices (D) after 5 days of control or Abemaciclib ex vivo treatment (n=5, respectively).

E. CD28 expression on CD8+ T cells in immunocompetent mice orthotopically injected with HP5712 (left) or 4T1 (right) tumor slices after 5 days of control or Abemaciclib treatment (n=5, respectively).

F-G. Representative IF images and quantifications (F; 3 areas × 3 samples, respectively) and 3D-IF images and quantifications (G; 3 areas × 3 samples, respectively) of F4/80 (green) and

CD8a (red) expressions on human Luminal breast tumor slices after 5 days of control or Abemaciclib treatment; scale bar = 100 μm**.**

Unpaired two-tailed t-tests (C-G), two-way ANOVA corrected for multiple comparisons (C, D). Error bars represent SD. *p<0.05, **p<0.01, ***p<0.001, ****p<0.0001.

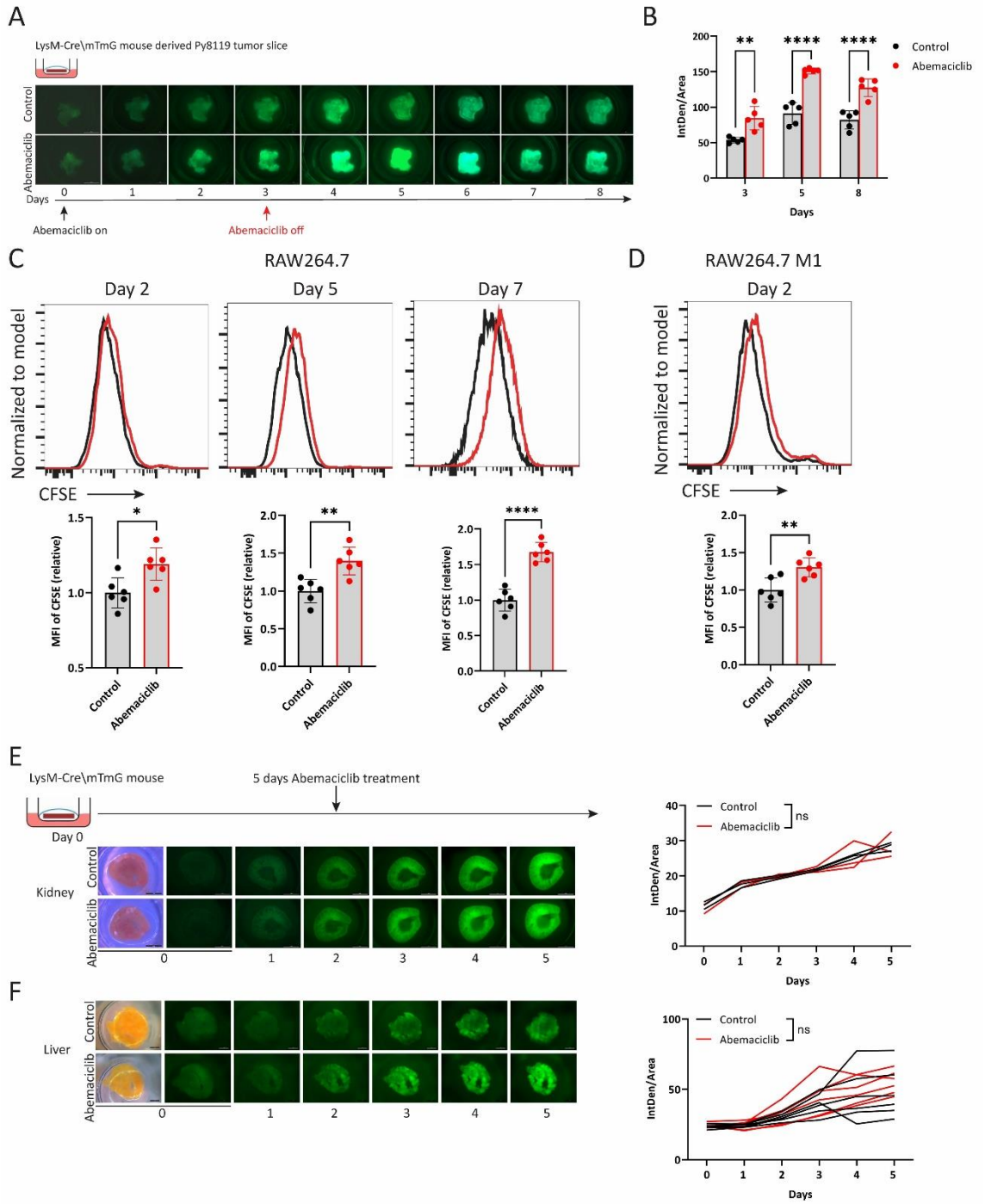

Supplementary Figure 4. CDK4/6 inhibition induces immune-like macrophage memory in a tumor-dependent manner.

A-B. Representative image (A) and intensity quantification at different days (B) of LysM-Cre\mTmG mice orthotopically injected with Py8119 tumor slices by control or Abemaciclib treatment (n=5, respectively); scale bar = 2 mm.

C. Representative FACS histograms and quantifications of CFSE expression on the surface of RAW264.7 macrophages after 2, 5, and 7 days of control or Abemaciclib treatment (n=6, respectively).
D. Representative FACS histograms and quantifications of CFSE expression on the surface of RAW264.7 (M1) macrophages after 2 days of control or Abemaciclib treatment (n=6, respectively).
E-F. Representative images and dynamic GFP signal intensity changes of LysM-Cre\mTmG tumor-free mice-derived kidney (E; n=5, respectively) and liver (F; n=5, respectively) slices after 5 days of control or Abemaciclib treatment; scale bar = 2 mm.
Unpaired two-tailed t-tests (C-F); two-way ANOVA corrected for multiple comparisons (B). Error bars represent SD. ns $p > 0.05$, *$p < 0.05$, ****$p < 0.0001$.

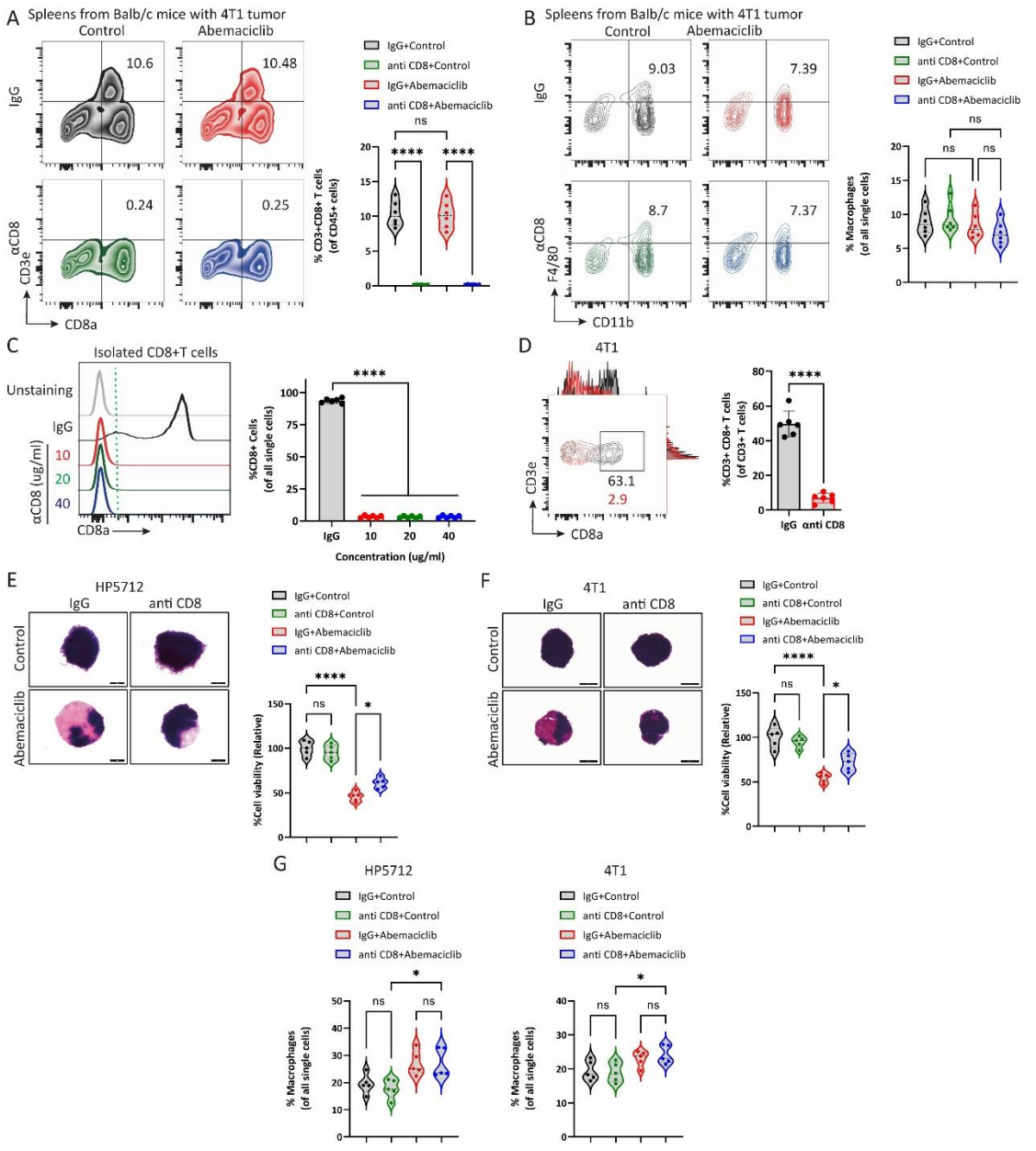

Supplementary Figure 5. CDK4/6 inhibition expands intratumoral macrophages ex vivo independent of CD8+ T cells.

A-B. Representative FACS plot and quantifications of CD8+ T cells (A) and macrophages (B) in spleens from Balb/c mice orthotopically injected with 4T1 cells after IgG or anti-CD8 depletion plus control or Abemaciclib treatment (n=6, respectively).

C. CD8a expression on FVB mice-derived naïve CD8+ T cells after IgG or gradient concentration of anti-CD8 depletion treatment (n=6, respectively).

D. Representative FACS plot and quantifications of CD8+ T cells in immunocompetent mice orthotopically injected with 4T1 tumor slices after IgG or anti-CD8 depletion ex vivo treatment (n=6, respectively).

E-F. Representative MTT images and quantification of cell viability in immunocompetent mice orthotopically injected with HP5712 (E; n=5, respectively) and 4T1 (F; n=5, respectively) after pre-IgG or pre-anti-CD8 plus control or Abemaciclib ex vivo treatment.

G. Intratumoral macrophages in immunocompetent mice orthotopically injected with HP5712 (left) and 4T1 (right) tumor slices after pre-IgG or pre-anti-CD8 plus control or Abemaciclib ex vivo treatment (n=5, respectively).

Unpaired two-tailed t-tests (D), one-way ANOVA corrected for multiple comparisons (A-C, E-G). Error bars represent SD. ns $p > 0.05$, *$p < 0.05$, **$p < 0.01$, ***$p < 0.001$, ****$p < 0.0001$.

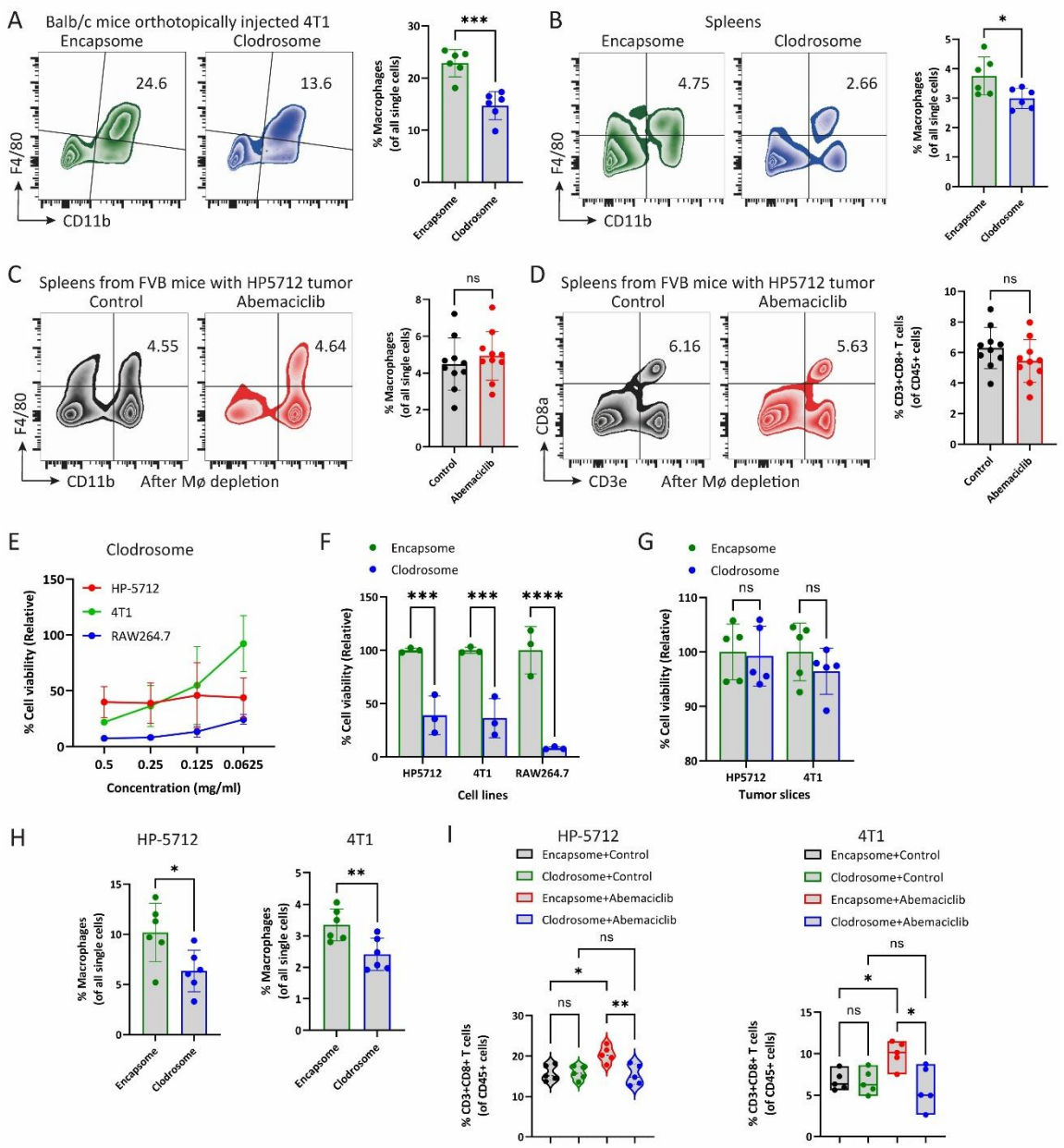

Supplementary Figure 6. CDK4/6 inhibition fails to expand intratumoral CD8+ T cells after macrophage depletion ex vivo.

A-B. Macrophage removal efficiency of Clodrosome in tumors (A) and spleens (B) from Balb/c mice orthotopically injected with 4T1 cells (n=6, respectively).

C-D. Representative FACS plot and quantifications of macrophages (C) and CD8+ T cells (D) in spleens from FVB mice orthotopically injected with HP5712 cells after Clodrosome plus control or Abemaciclib treatment (n=10, respectively).

E. Cell viability of cancer cells and macrophages after gradient concentration of Encapsome or Clodrosome treatment (n=3, respectively).

F-G. Cell viability of cell lines (F; n=3, respectively) and immunocompetent mice orthotopically injected with tumor slices (G; n=5, respectively) after 0.25 mg/ml Encapsome or Clodrosome treatment.

H. Intratumoral macrophages in immunocompetent mice orthotopically implanted with HP5712 (left) and 4T1 (right) tumor slices after Encapsome or Clodrosome treatment (n=6, respectively).

I. Intratumoral CD8+ T cells from immunocompetent mice orthotopically implanted with HP5712 (left) and 4T1 (right) tumor slices after Encapsome or Clodrosome pretreatment plus control or Abemaciclib treatment (n=5, respectively).

Unpaired two-tailed t-tests (A-D, H), one-way ANOVA corrected for multiple comparisons (I), two-way ANOVA corrected for multiple comparisons (F, G). Error bars represent SD. ns $p > 0.05$, *$p < 0.05$, **$p < 0.01$, ***$p < 0.001$, ****$p < 0.0001$.

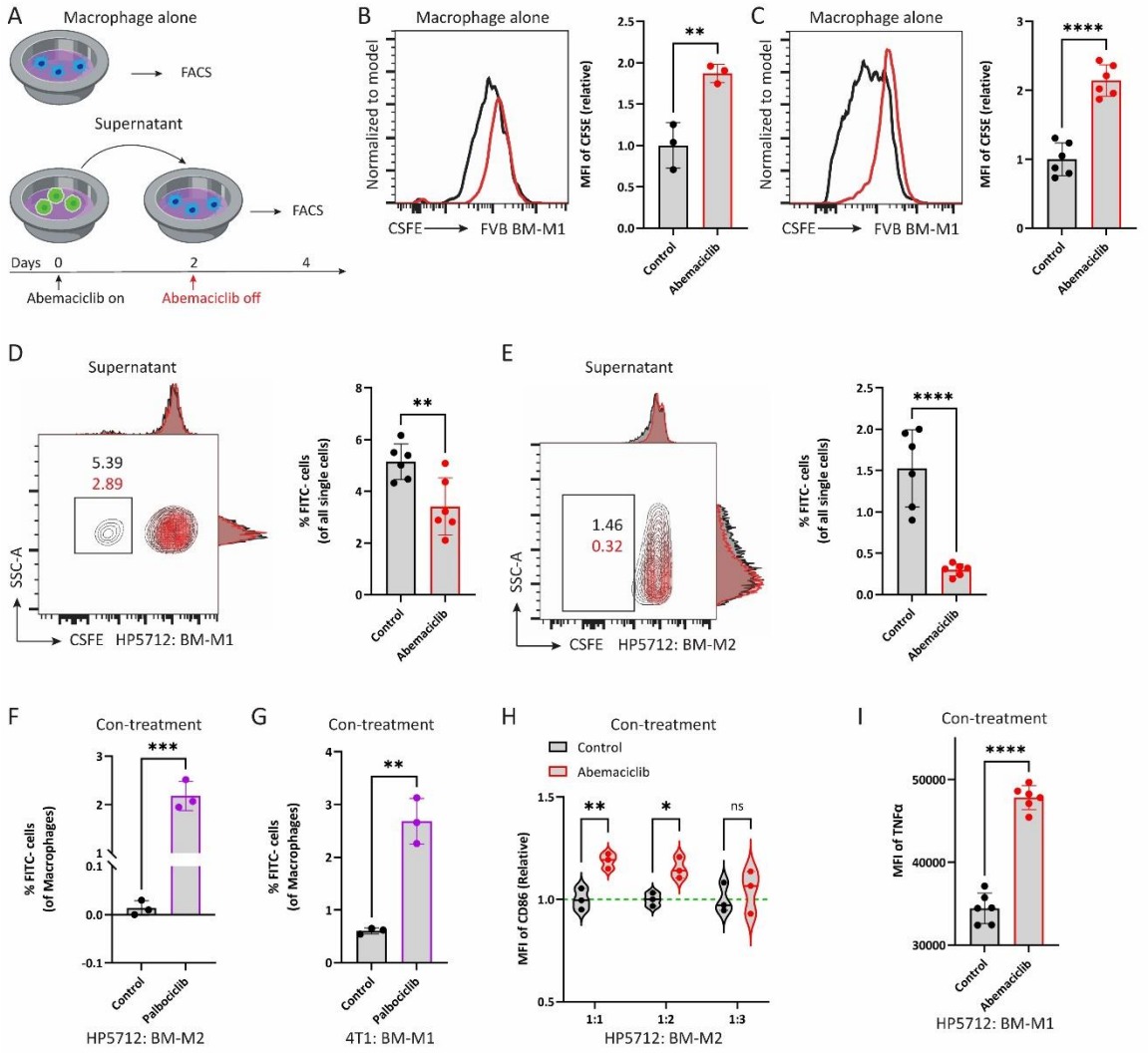

Supplementary Figure 7. CDK4/6 inhibition increases macrophage proliferation and activation and polarizes M2 to M1 macrophages dependent on the tumor microenvironment.

A. Macrophage alone or the supernatant model to detect macrophage proliferation and activation potential.

B-C. Representative FACS histograms and quantifications of the proliferation potential of FVB mice BM-M1 macrophages (B; n=3, respectively) or BM-M2 macrophages (C; n=6, respectively) alone after control or Abemaciclib treatment.

D-E. Representative FACS plots and quantifications of the proliferation potential of FVB mice BM-M1 macrophages (D; n=6, respectively) or BM-M2 macrophages (E; n=6, respectively) in the supernatant model after control or Abemaciclib treatment.

F-G. Quantifications of the proliferation potential of FVB mice BM-M2 macrophages cocultured with HP-5712 (F; n=3, respectively) or Balb/c mice BM-M1 macrophages cocultured with 4T1 (G; n=3, respectively) after control or Palbociclib treatment in the con-treatment model.

H. Fold changes of CD86 expressions on the surface of FVB mice BM-M2 macrophages cocultured with HP5712 at different ratios after control or Abemaciclib treatment in the con-treatment model (n=3, respectively).

I. Quantifications of TNFα expressions of FVB mice BM-M1 macrophages cocultured with HP5712 after control or Abemaciclib treatment in the con-treatment model (n=6, respectively).

Unpaired two-tailed t-tests (B-G, I), two-way ANOVA corrected for multiple comparisons (H). Error bars represent SD. *$p<0.05$, **$p<0.01$, ***$p<0.001$, ****$p<0.0001$.

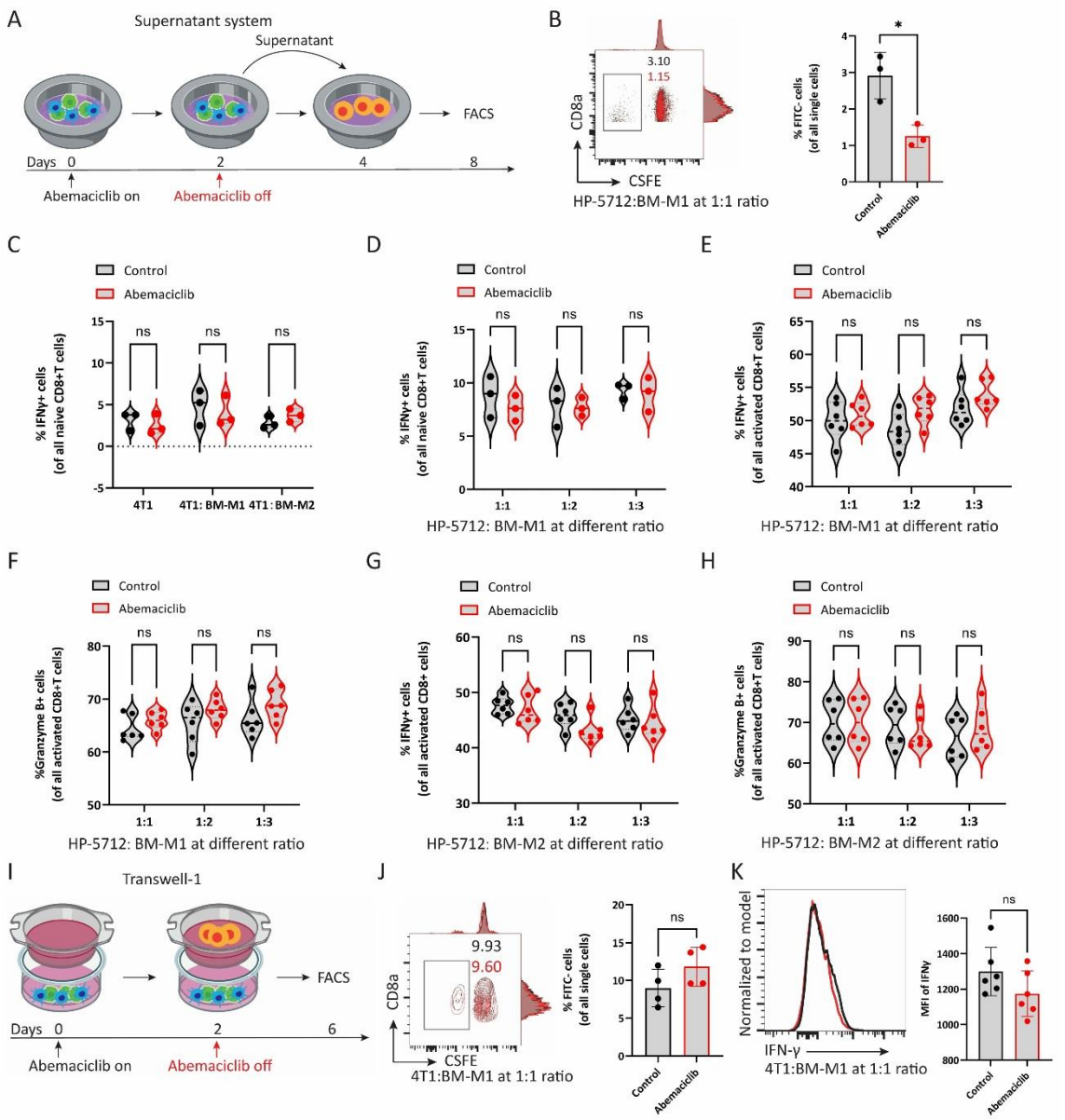

Supplementary Figure 8. CDK4/6 inhibition-trained M1 tumor-associated macrophage supernatant fails to stimulate CD8+ T cell antitumor immunity without cell-cell interactions.

A. The supernatant model to detect CD8+ T cell proliferation and activation.

B. Representative FACS plots and quantifications of the proliferation potential of Balb/c mice-derived naïve CD8+ T cells in the supernatant model after control or Abemaciclib treatment (n=3, respectively).

C. Quantifications of IFNγ expressions on the surface of FVB mice-derived naïve CD8+ T cells in the supernatant model of HP5712 cocultured with FVB mice BM-M1 macrophages at different ratios after control or Abemaciclib treatment (n=3, respectively).

D. Quantifications of IFNγ expressions on the surface of Balb/c mice-derived naïve CD8+ T cells in the supernatant model of 4T1 alone, 4T1 cocultured with Balb/c mice BM-M1 or BM-M2 macrophages at a 1:1 ratio after control or Abemaciclib treatment (n=3, respectively).

E-F. Quantifications of IFNγ (E; n=6, respectively) and granzyme B (F; n=6, respectively) expressions on the surface of FVB mice-derived activated CD8+ T cells in the supernatant model of HP5712 cocultured with FVB mice BM-M1 macrophages at different ratios after control or Abemaciclib treatment.

G-H. Quantifications of IFNγ (G; n=6, respectively) and granzyme B (H; n=6, respectively) expressions on the surface of FVB mice-derived activated CD8+ T cells in the supernatant model of HP5712 cocultured with FVB mice BM-M2 macrophages at different ratios after control or Abemaciclib treatment.

I. The Transwell model to detect CD8+ T cell proliferation and activation.

J. Representative FACS plots and quantifications of the proliferation potential of Balb/c mice-derived naïve CD8+ T cells in the Transwell model after control or Abemaciclib treatment (n=3, respectively).

K. Representative FACS histograms and quantifications of IFNγ expressions on the surface of Balb/c mice-derived activated CD8+ T cells in the supernatant model of 4T1 cocultured with Balb/c mice BM-M1 macrophages at a 1:1 ratio after control or Abemaciclib treatment.

Unpaired two-tailed t-tests (B, J, K), two-way ANOVA corrected for multiple comparisons (C-H). Error bars represent SD. ns $p > 0.05$, *$p < 0.05$.

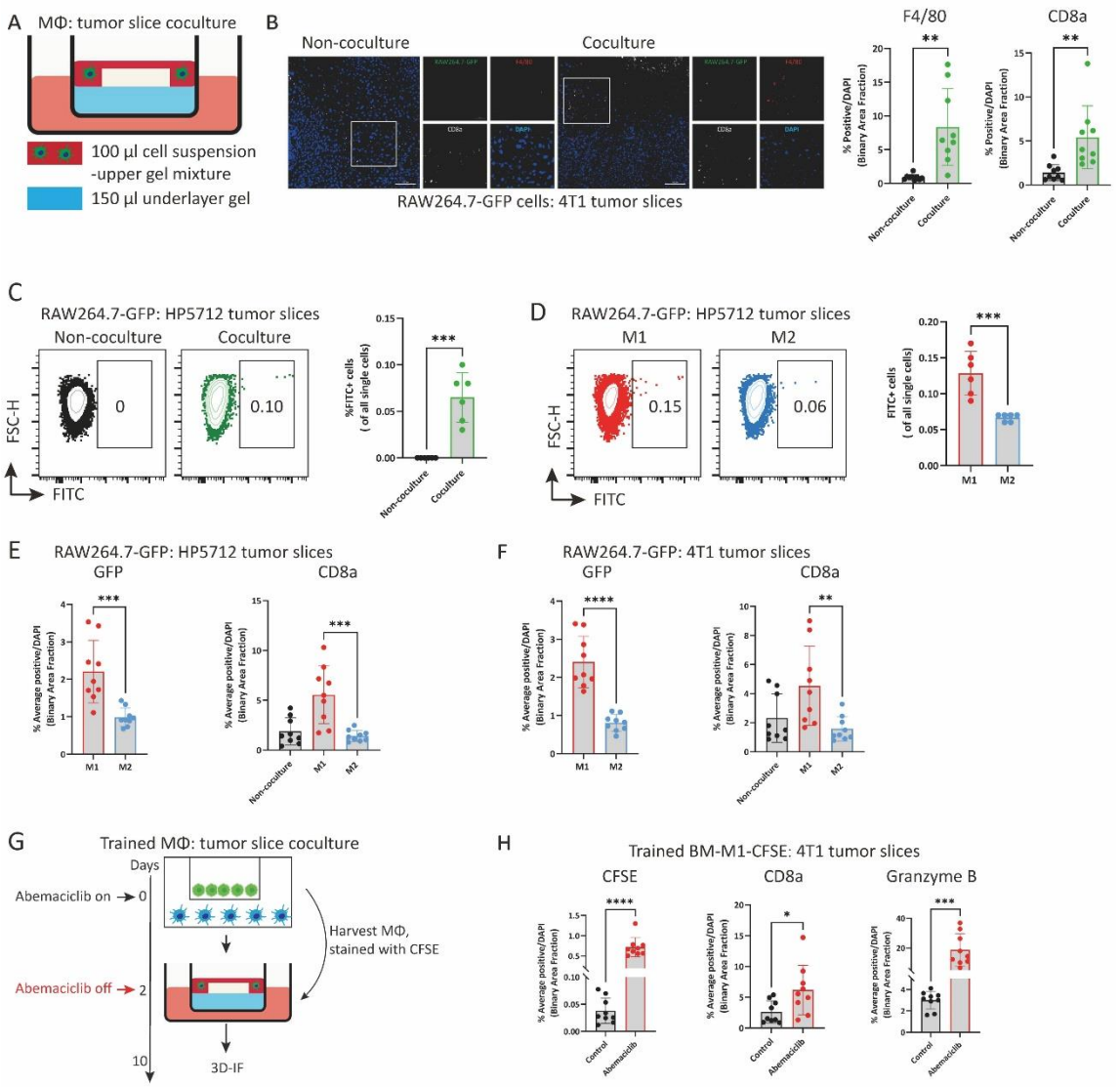

Supplementary Figure 9. CDK4/6 trained M1 tumor-associated macrophages penetrate into tumor slices and remodel the tumor immune microenvironment.

A. Coculture model of macrophages and tumor slices.

B. Representative IF images and quantifications of penetrated RAW264.7-GFP (green) and F4/80 (red) and CD8a (white) expressions on the surfaces of Balb/c mice orthotopically injected with 4T1 tumor slices after 8 days of coculture (3 areas × 3 samples, respectively).

C. Representative FACS plots and quantifications of RAW264.7-GFP penetration capacity in FVB mice orthotopically injected with HP5712 tumor slices after 8 days of coculture (n=6, respectively).

D. Penetration capacity of different RAW264.7-GFP subpopulations in FVB mice orthotopically injected with HP5712 tumor slices after 8 days of coculture (n=6, respectively).

E-F. Quantification of penetration capacity of RAW264.7-GFP M1 or M2 macrophages and CD8a expressions in immunocompetent mice orthotopically injected with HP5712 (E; 3 areas × 3 samples, respectively) or 4T1 (F; 3 areas × 3 samples, respectively) tumor slices after 8 days of coculture.

G. Workflow to detect penetration capacity of Abemaciclib-trained immunocompetent mice BM-M1 in tumor slices and intratumoral immune cell repertoire changes after coculture.

H. Quantification of CFSE, CD3/CD8, and granzyme B expressions in Balb/c mice orthotopically injected with 4T1 tumor slices cocultured with control or Abemaciclib-trained BM-M1-CFSE (3 areas × 3 samples, respectively).

Unpaired two-tailed t-tests (B-F, H); one-way ANOVA corrected for multiple comparisons (E, F). Error bars represent SD. *p<0.05, **p<0.01, ***p<0.001, ****p<0.0001.

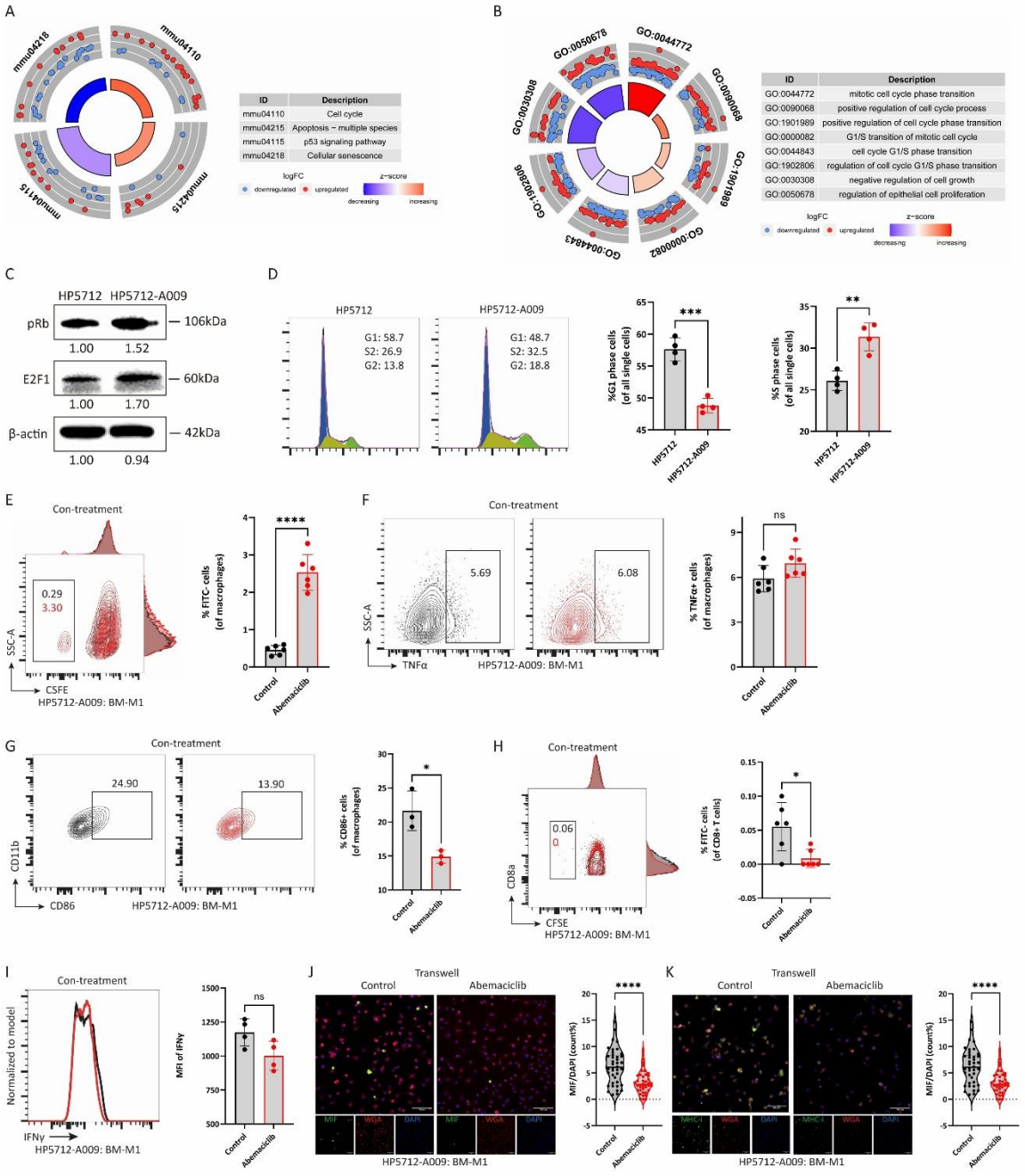

Supplementary Figure 10. CDK4/6 inhibition fails to reprogram tumor-associated macrophages and trigger CD8+ T cell antitumor immunity in CDK4/6 resistant tumor cells.

A-B. KEGG terms (A) and GO terms (B) of significantly upregulated and downregulated genes in HP5712-A009 cells compared to HP5712 cells during the log phase (n=3, respectively).

C. Representative immunoblots of pRb and E2F1 expressions in HP5712-A009 and HP5712 cells during the log phase.

D. Representative FACS cell cycle distribution and quantifications of G1 and S phase cell populations between HP5712-A009 and HP5712 during the log phase (n=4, respectively).

E-G. Representative FACS plots and quantifications of proliferation potential of FVB mice BM-M1 macrophages (E; n=6, respectively), TNFα expressions on the surface of FVB mice BM-M1 macrophages (F; n=6, respectively), and CD86 expressions on the surface of FVB mice BM-M2 macrophages (G; n=3, respectively) cocultured with HP5712-A009 cells after control or Abemaciclib treatment in the con-treatment model.

H. Representative FACS plots and quantifications of proliferation potential of FVB mice-derived naïve CD8+ T cells in the coculture system of HP5712-A009: FVB mice BM-M1 macrophages at a 1:1 ratio after vehicle or Abemaciclib treatment (n=6, respectively).

I. Representative FACS histograms and quantifications of IFNγ expressions on FVB mice-derived activated CD8+ T cells in the coculture system of HP5712-A009: FVB mice BM-M1 macrophages at a 1:1 ratio after vehicle or Abemaciclib treatment (n=4, respectively).

J. Representative images and quantifications of MIF expression (green) in control- or Abemaciclib-treated FVB mice BM-M1 macrophage from HP5712-A009: BM-M1 in the Transwell model (10 areas × 4 samples, respectively); scale bar = 100 μm.

K. Representative images and quantifications of MHC-I expression (green) in control- or Abemaciclib-treated FVB mice BM-M1 macrophages from HP5712-A009: BM-M1 in the Transwell model (10 areas × 4 samples, respectively); scale bar = 100 μm.

Unpaired two-tailed t-tests (D-K). Error bars represent SD. ns $p > 0.05$, *$p < 0.05$, **$p < 0.01$, ***$p < 0.001$, ****$p < 0.0001$.

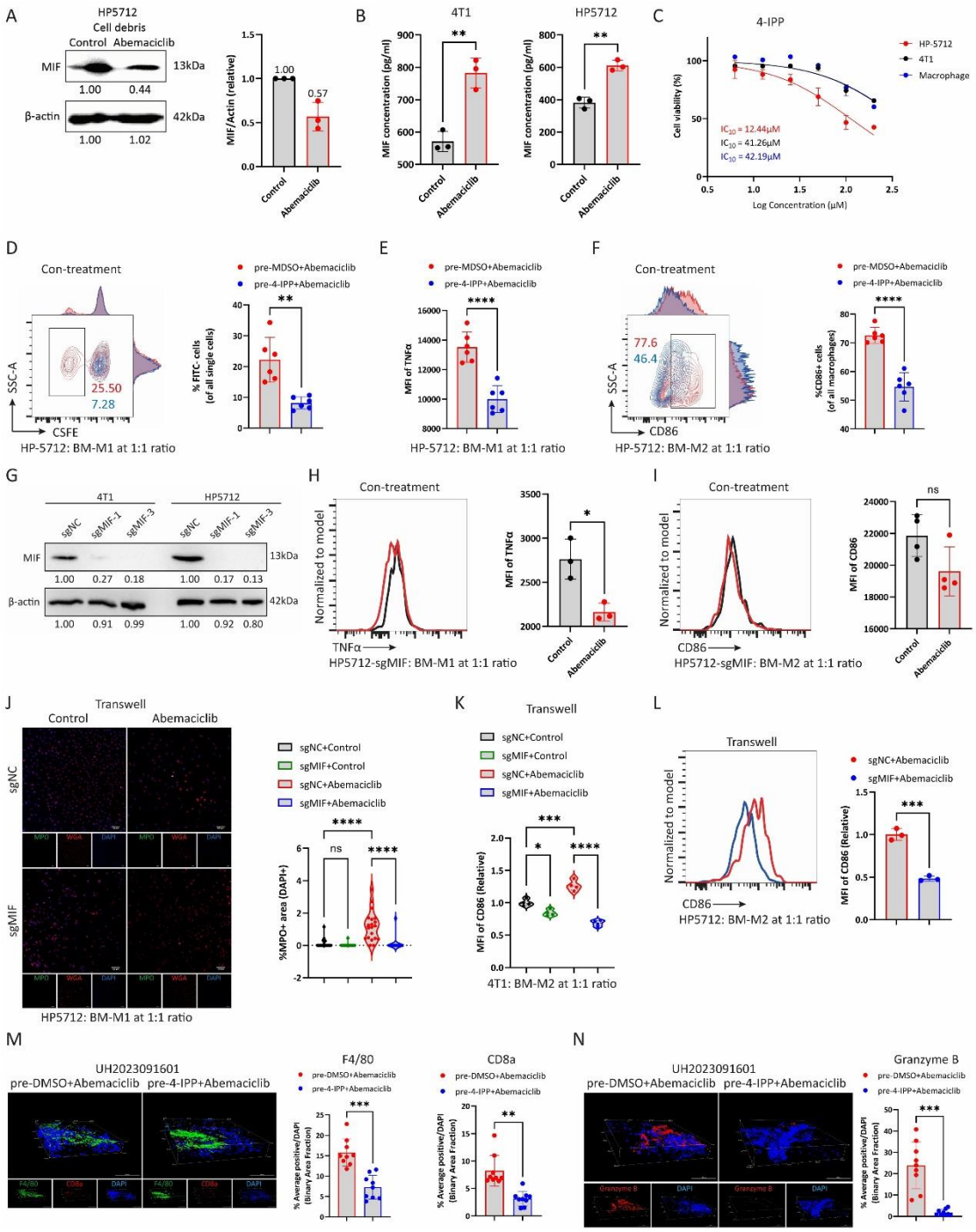

Supplementary Figure 11. Tumor cell-secreted MIF is important to CDK4/6 inhibition reprogramming tumor-associated macrophages.

A. Representative immunoblots and fold changes of MIF expressions in HP5712 cell debris after control or Abemaciclib treatment (n=3, respectively).

B. Secreted MIF concentration in the supernatant from 4T1 and HP5712 cells after control or Abemaciclib treatment (n=3, respectively).

C. IC10 of 4-IPP on HP5712, 4T1, and FVB mice BM-M1 macrophages (n=3, respectively).

D. Representative FACS plots and quantifications of the proliferation potential of FVB mice BM-M1 macrophages cocultured with HP5712 after pre-DMSO plus Abemaciclib or pre-4-IPP plus Abemaciclib treatment in the con-treatment model (n=6, respectively).

E. Quantifications of TNFα expressions on the surface of FVB mice BM-M1 macrophages cocultured with HP5712 after pre-DMSO plus Abemaciclib or pre-4-IPP plus Abemaciclib treatment in the con-treatment model (n=6, respectively).
F. Representative FACS plots and quantifications of CD86 expressions on the surface of FVB mice BM-M1 macrophages cocultured with HP5712 after pre-DMSO plus Abemaciclib or pre-4-IPP plus Abemaciclib treatment in the con-treatment model (n=6, respectively).
G. Knockout efficacy of two different sgMIFs on MIF expression in 4T1 (left) and HP5712 (right) cell lines.
H. Representative FACS histograms and quantifications of TNFα expressions on the surface of FVB mice BM-M1 macrophages cocultured with HP5712-sgMIF after control or Abemaciclib treatment in the con-treatment model (n=3, respectively).
I. Representative FACS histograms and quantifications of CD86 expressions on the surface of FVB mice BM-M2 macrophages cocultured with HP5712-sgMIF after control or Abemaciclib treatment in the con-treatment model (n=4, respectively).
J. Representative images and quantifications of MPO expressions (green) in FVB mice BM-M1 macrophages cocultured with HP5712-sgNC or HP5712-sgMIF after control or Abemaciclib treatment in the Transwell model (5 areas × 4 samples, respectively); scale bar=100μm.
K. Quantifications of CD86 expressions on the surface of Balb/c mice BM-M2 macrophages cocultured with 4T1-sgNC or 4T1-sgMIF after control or Abemaciclib treatment in the Transwell model (n=4, respectively).
L. Representative FACS histograms and quantifications of CD86 expressions on the surface of FVB mice BM-M2 macrophages cocultured with HP5712-sgNC or HP5712-sgMIF after Abemaciclib treatment in the Transwell model (n=3, respectively).
M-N. Representative 3D-IF images and quantifications of F4/80 (green) and CD8a (red) (M) and granzyme B (red) (N) expressions in human Luminal breast tumor slices after pre-DMSO plus Abemaciclib or pre-4-IPP plus Abemaciclib treatment (3 areas × 3 samples, respectively); scale bar=100μm.
Unpaired two-tailed t-tests (B, D-F, H, I, L-N); one-way ANOVA corrected for multiple comparisons (J, K). Error bars represent SD. ns $p > 0.05$, *$p < 0.05$, **$p < 0.01$, ***$p < 0.001$, ****$p < 0.0001$.

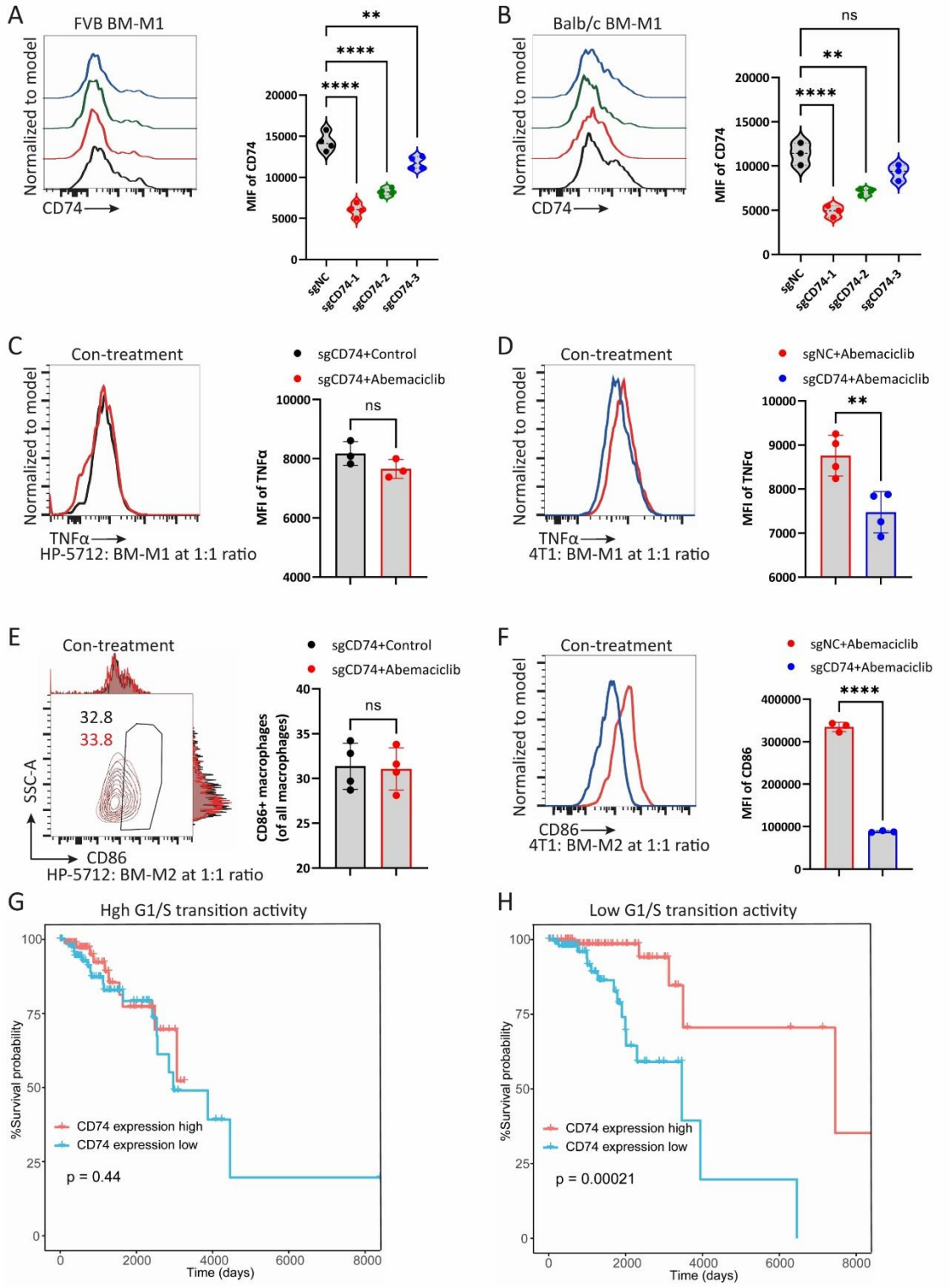

Supplementary Figure 12. CD74 deletion on macrophages blocks the functional reprogramming of tumor-associated macrophages by CDK4/6 inhibition

A-B. Knockout efficacy of three different sgCD74s on CD74 expressions in FVB (A; n=4, respectively) and Balb/c (B; n=3, respectively) mice BM-M1 macrophages.

C. Representative FACS histograms and quantifications of TNFα expressions on the surface of FVB mice BM-M1-sgCD74 macrophages cocultured with HP5712 after control or Abemaciclib treatment in the con-treatment model (n=3, respectively).

D. Representative FACS histograms and quantifications of TNFα expressions on the surface of Balb/c mice BM-M1-sgNC or sgCD74 macrophages cocultured with 4T1 after Abemaciclib treatment in the con-treatment model (n=4, respectively).
E. Representative FACS plots and quantifications of CD86 expressions on the surface of FVB mice BM-M2-sgCD74 macrophages cocultured with HP5712 after control or Abemaciclib treatment in the con-treatment model (n=4, respectively).
F. Representative FACS histograms and quantifications of CD86 expressions on the surface of Balb/c mice BM-M2-sgNC or sgCD74 macrophages cocultured with 4T1 after Abemaciclib treatment in the con-treatment model (n=3, respectively).
G-H. TCGA analysis of survival benefits between CD74-high and CD74-low breast cancer patients in high G1/S transition activity cohort (G) and low G1/S transition activity cohort (H), respectively.
Unpaired two-tailed t-tests (C-F); one-way ANOVA corrected for multiple comparisons (A-B). Error bars represent SD. ns $p > 0.05$, **$p < 0.01$, ****$p < 0.0001$.

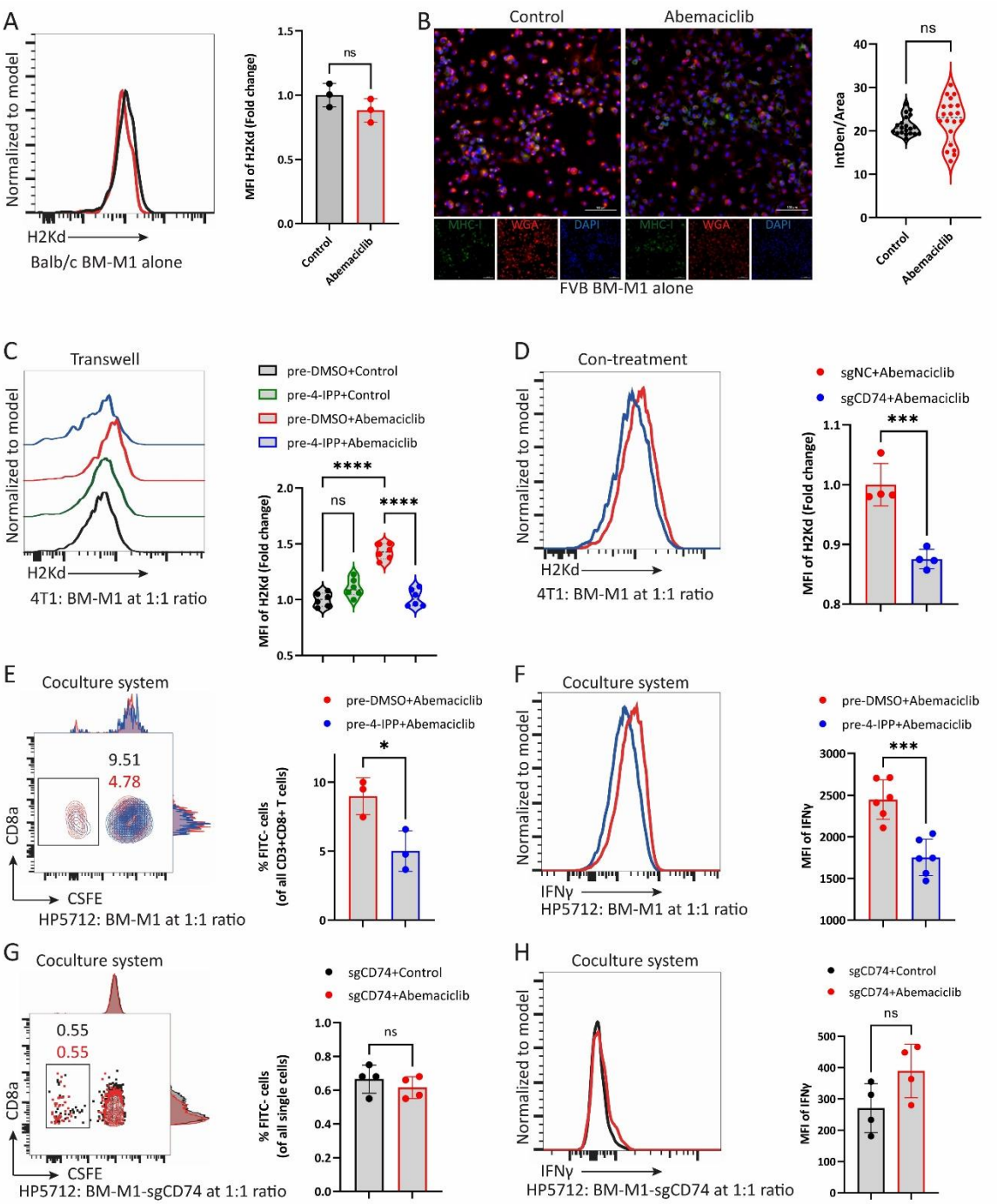

Supplementary Figure 13. CDK4/6 inhibition-induced MIF dominates MHC-I antigen presentation machinery on M1 tumor-associated macrophages

A. Representative FACS histograms and quantifications of H2Kd expressions on Balb/c mice BM-M1 macrophages after control or Abemaciclib treatment (n=3, respectively).

B. Representative images and quantifications of MHC-I expression (green) on FVB mice BM-M1 macrophages after control or Abemaciclib treatment (5 areas × 4 samples, respectively); scale bar=100μm.

C. Representative FACS histograms and quantifications of H2Kd expressions on Balb/c mice BM-M1 macrophages co-cultured with 4T1 after pre-DMSO or 4-IPP plus control or Abemaciclib treatment in the Transwell model (n=6, respectively).

D. Representative FACS histograms and quantifications of H2Kd expressions on Balb/c mice BM-M1-sgNC or sgCD74 macrophages co-cultured with 4T1 after Abemaciclib treatment in the co-treatment model (n=4, respectively).
E. Representative FACS plots and quantifications of the proliferation potential of FVB mouse-derived naïve CD8+ T cells in the co-culture system of HP5712: FVB mice BM-M1 macrophages at a 1:1 ratio after pre-DMSO plus Abemaciclib or 4-IPP plus Abemaciclib treatment (n=3, respectively).
F. Quantifications of IFNγ expressions on FVB mouse-derived activated CD8+ T cells in the co-culture system of HP5712: FVB mice BM-M1 macrophages at a 1:1 ratio after pre-DMSO plus Abemaciclib or 4-IPP plus Abemaciclib treatment (n=6, respectively).
G. Representative FACS plots and quantifications of the proliferation potential of FVB mouse-derived naïve CD8+ T cells in the co-culture system of HP5712: FVB mice BM-M1-sgCD74 macrophages at a 1:1 ratio after control or Abemaciclib treatment (n=4, respectively).
H. Representative FACS histograms and quantifications of IFNγ expressions on FVB mouse-derived activated CD8+ T cells in the co-culture system of HP5712: FVB mice BM-M1-sgCD74 macrophages at a 1:1 ratio after control or Abemaciclib treatment (n=4, respectively).
Unpaired two-tailed t-tests (A, B, D-H); one-way ANOVA corrected for multiple comparisons (C). Error bars, SD. ns $p > 0.05$, *$p < 0.05$, **$p < 0.01$, ***$p < 0.001$, ****$p < 0.0001$.

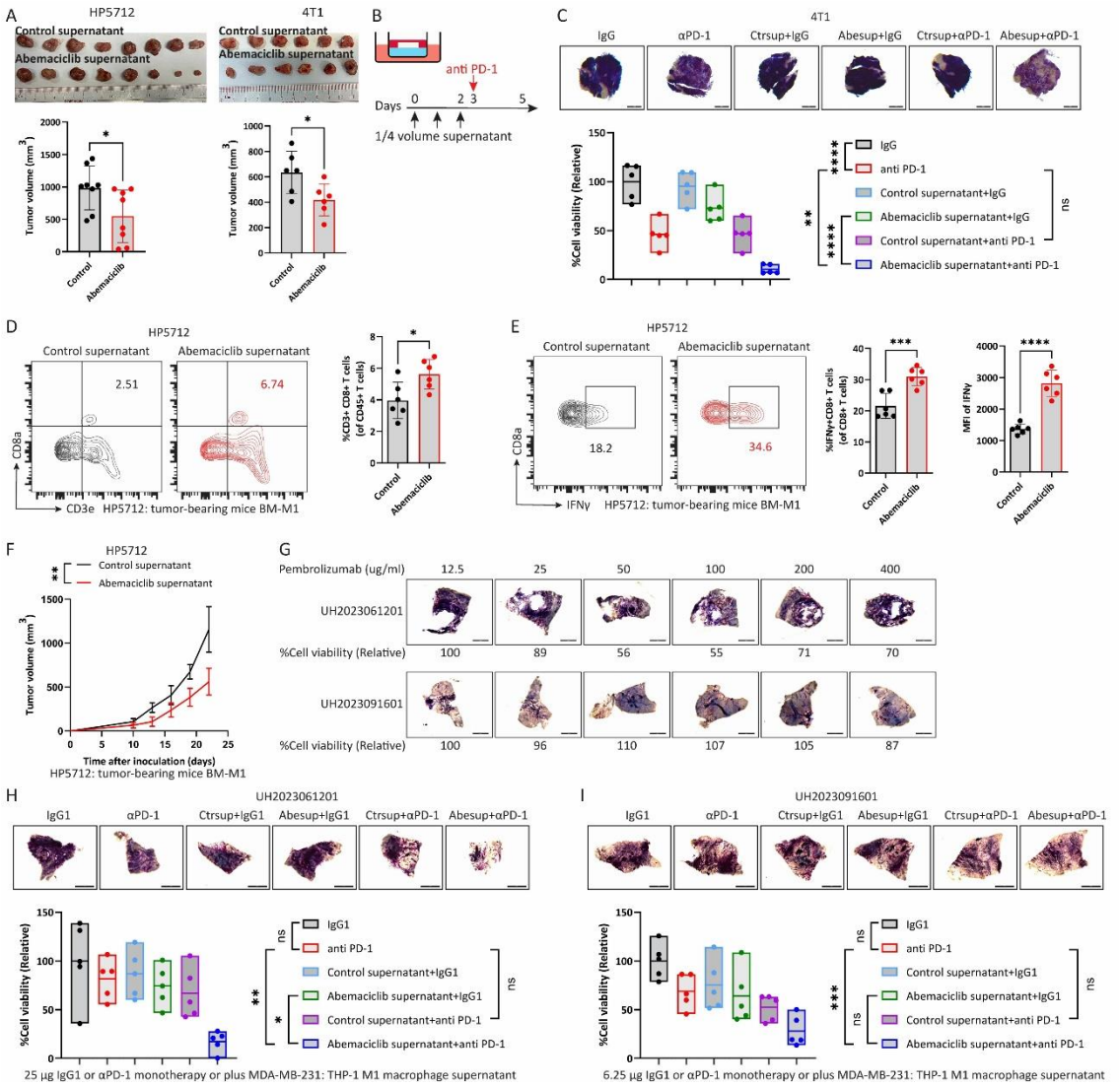

Supplementary Figure 14. CDK4/6 inhibition-trained M1 tumor-associated macrophage supernatant therapy augments tumor response of PD-1 ICB therapy ex vivo.

A. Representative tumor images and tumor volume comparison of FVB mice orthotopically injected with HP5712 cells (left; n=8, respectively) and Balb/c mice orthotopically injected with 4T1 cells (right; n=6, respectively) after 7 days of control supernatant or Abemaciclib supernatant therapy.

B. Workflow of CDK4/6 inhibition-trained M1 tumor-associated macrophage supernatant therapy combined with PD-1 ICB therapy ex vivo.

C. Representative MTT images and quantification of cell viability in Balb/c mice orthotopically injected with 4T1 tumor slices after IgG or αPD-1 alone or combined with control supernatant or Abemaciclib supernatant therapy (n=6, respectively); scale bar=2mm.

D. Representative FACS plot and quantifications of intratumoral CD8+ T cells from FVB mice orthotopically injected with HP5712 cells after control supernatant or Abemaciclib supernatant therapy (n=6, respectively).

E. Representative FACS plot and quantifications of IFNγ expressions on the surface of intratumoral CD8+ T cells from FVB mice orthotopically injected with HP5712 cells after control supernatant or Abemaciclib supernatant therapy (n=6, respectively).

F. Tumor volume changes of FVB mice orthotopically injected with HP5712 cells after 7 days of control supernatant or Abemaciclib supernatant therapy (n=6, respectively); D-F, the BM-M1 macrophages were derived from FVB mice orthotopically injected with HP5712 cells at day-7.

G. Tumor response of human TNBC and Luminal breast tumor slices to gradient concentrations of Pembrolizumab; scale bar=2mm.

H. Representative MTT images and quantification of cell viability in human TNBC slices after 25 μg/ml IgG1 or Pembrolizumab alone or combined with control supernatant or Abemaciclib supernatant therapy (n=5, respectively); scale bar=2mm.

I. Representative MTT images and quantification of cell viability in human Luminal breast tumor slices after 6.25 μg/ml IgG1 or Pembrolizumab alone or combined with control supernatant or Abemaciclib supernatant therapy (n=5, respectively); H-I, the supernatant was collected from MDA-MB-231 cells cocultured with THP1 M1 macrophages at a 1:1 ratio after control or Abemaciclib treatment; scale bar=2mm.

Unpaired two-tailed t-tests (A, D-F); one-way ANOVA corrected for multiple comparisons (C, H-I). Error bars, SD. ns $p > 0.05$, *$p < 0.05$, **$p < 0.01$, ***$p < 0.001$, ****$p < 0.0001$.